

CHAPTER 7

THE MAIN RING IN TEVATRON I7.1 Functions of the Main Ring in Tevatron I

The Main Ring is required to perform five separate functions in the Tevatron I mode:

1. Acceleration of protons for antiproton production. During antiproton production and accumulation, the Main Ring will be required to accelerate single batches of protons (approx. 82 bunches) of intensity greater than 2×10^{12} protons per batch to 120 GeV. This will be done routinely on a 2-sec cycle. Each of these acceleration cycles must include the bunch-narrowing technique and extraction at F17 described in Chapter 2.

During this mode of operation, a special low-level rf system must be used. This system will contain provision for transient beam-loading compensation. In addition, the technique for phase-locking the Main Ring to the Booster will be slightly different from that used during fixed-target operation.

2. Injection of \bar{p} 's from the Accumulator into the Main Ring. Bunches of antiprotons containing 10^{11} \bar{p} 's must be transported to the Main Ring and injected.

3. Acceleration of antiprotons to 150 GeV. After a sufficient number and density of antiprotons have been established in the Accumulator, the Main Ring must be used to accelerate groups of antiproton bunches to 150 GeV. This acceleration cycle must include the bunch manipulations at 150 GeV described in Sections 6.1 and 6.2. Special additions to the rf systems will be required to accomplish these manipulations. Following these acceleration cycles, the single antiproton bunches must be extracted at E0 for injection into the Tevatron.

4. Acceleration of protons to 150 GeV. The Main Ring will be required to accelerate a few bunches of protons to 150 GeV, where they will be combined to form single proton bunches containing 10^{11} protons. This operation will be similar in many respects to the antiproton acceleration described above and the same special additions to the rf systems will be utilized.

5. Transfer of particles from the Main Ring into the Energy Saver. Transfers of 150 GeV protons and antiprotons are both described in Chapter 8.

7.2 Antiproton Injection

The antiproton bunches from the Accumulator are matched into the proton extraction line at EB5. They are then transported back down the 120-GeV extraction line and injected into the Main Ring at the F17 Lambertson. Special low-current power supplies are used to power the 120-GeV extraction line to ease regulation problems caused by running large power supplies at 5% levels.

The orbit excursions of the injected beam between F17 and E48 are limited by a 4-bump centered at F0 (produced by the horizontal correction dipoles at E48, E49, F11 and F13.) An additional orbit bump centered at F17 (produced by the correction dipoles at F15, F17, F19 and F22) may be used to steer the beam up to 14 mm away from the Lambertson septum on the first turn, if this is necessary. These bumps will be on at pbar injection time, and will probably be left on throughout the acceleration cycle.

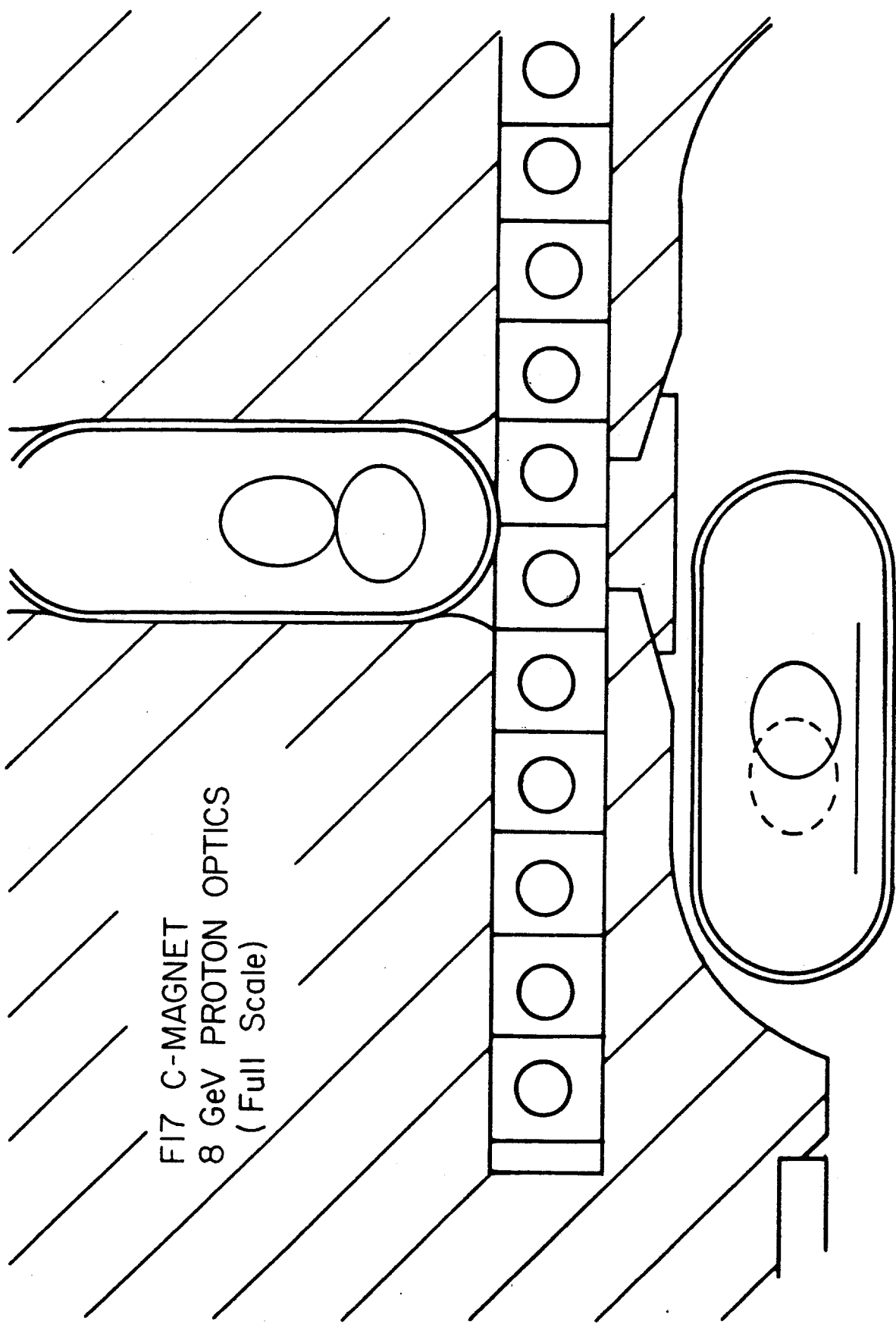
The kicker will be a copy of one module (40 in.) of the Main Ring C48-style magnet. The necessary kick angle of approximately 450 μ rad requires approximately 500 A. The pulser will be a simple SCR-switched capacitive discharge type, producing a half-sine-wave of falltime approximately 15 μ sec. Flat top uniformity of approximately $\pm 0.01\%$ for approximately 350 msec is expected.

The following calculations have been done for a momentum of 8.89 GeV/c, emittance (at that energy) of 2 pi mm-mrad, and a momentum spread of $\pm 0.09\%$.

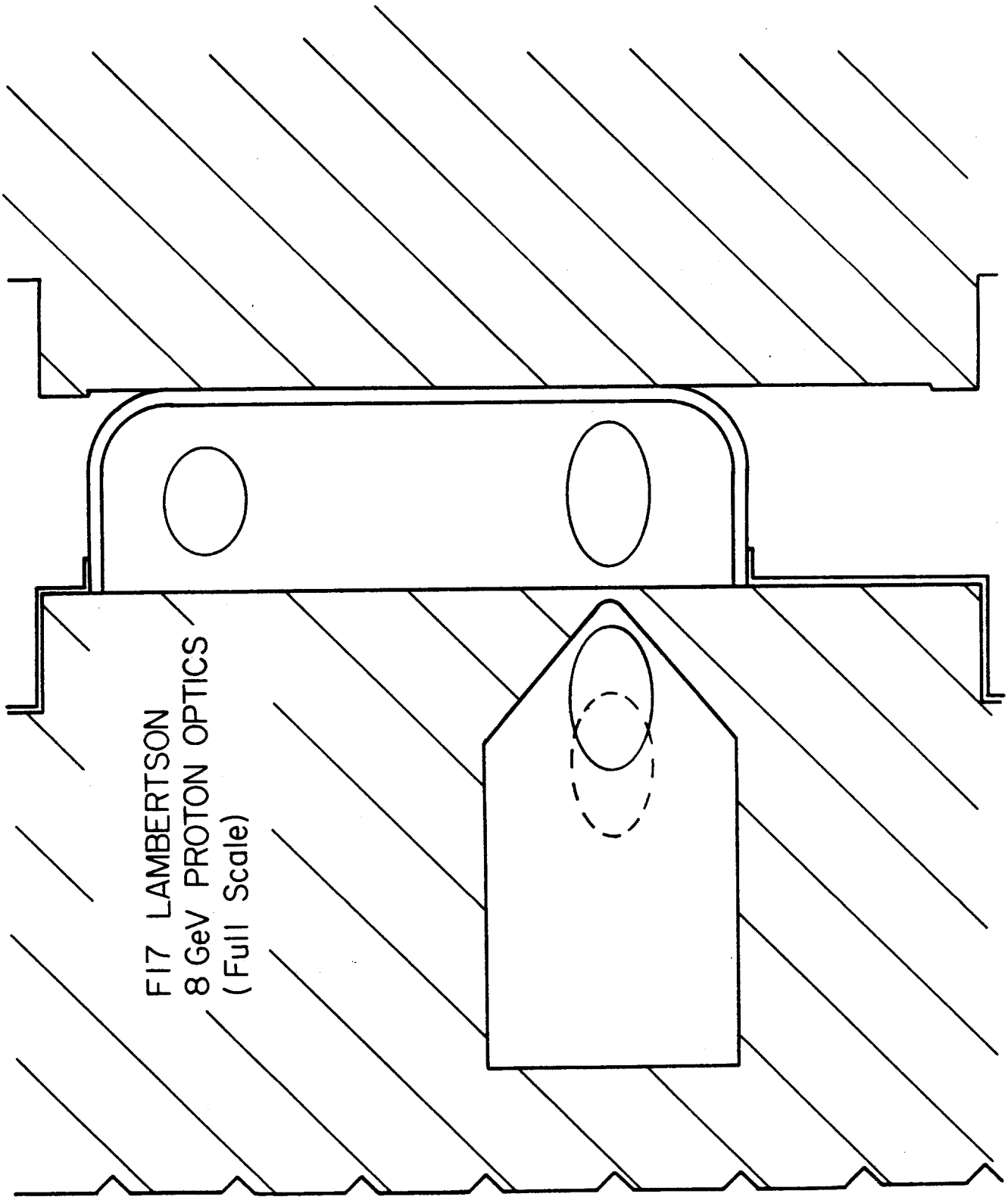
Figures 7-1, 7-2 and 7-3 show the injected beam spot at the C-magnet, Lambertsons, and the F17-1 quad. In the figures, the dotted line indicates the beam spot for the circulating beam with the F17 steering bump on at maximum (14 mm). For the injected beam, the closest clearance in the Lambertson aperture is 3 mm (on both sides,) and also 3 mm at the F17-1 quad.

Figure 7-4 shows the orbit produced by the kicker at E48 alone; Fig. 7-5 shows the kicker plus the kick-offsetting bump at F0; and Fig. 7-6 shows the injected orbit and the F17 bump which may be used to steer the beam away from the septum on the first turn after injection.

Figure 7-7 shows the region near F17 in detail, indicating both the circulating and injected beam envelopes. Nearly the full inner limits of the physical aperture of the quad at F17-1 and the dipoles at F16-7 are explored.



FI7 C-MAGNET
8 GeV PROTON OPTICS
(Full Scale)



F17 LAMBERTSON
8 GeV PROTON OPTICS
(Full Scale)

Figure 7-2

8 GeV PROTONS
F 17-1 QUAD
(Full Scale)

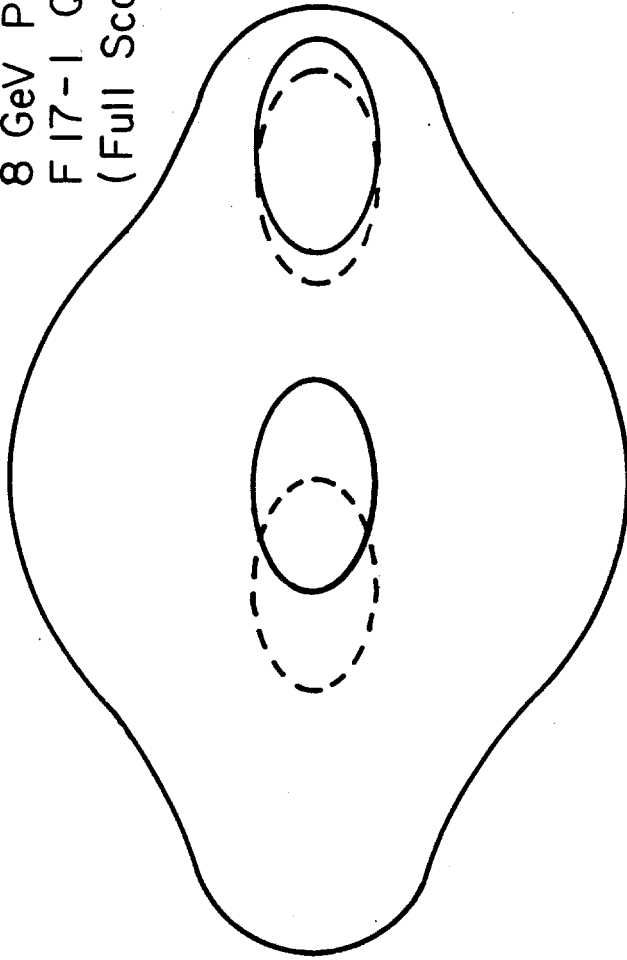


Figure 7-3

TUNE 19.400
MAX. OFFSET 4.37
HORIZONTAL PROJECTION

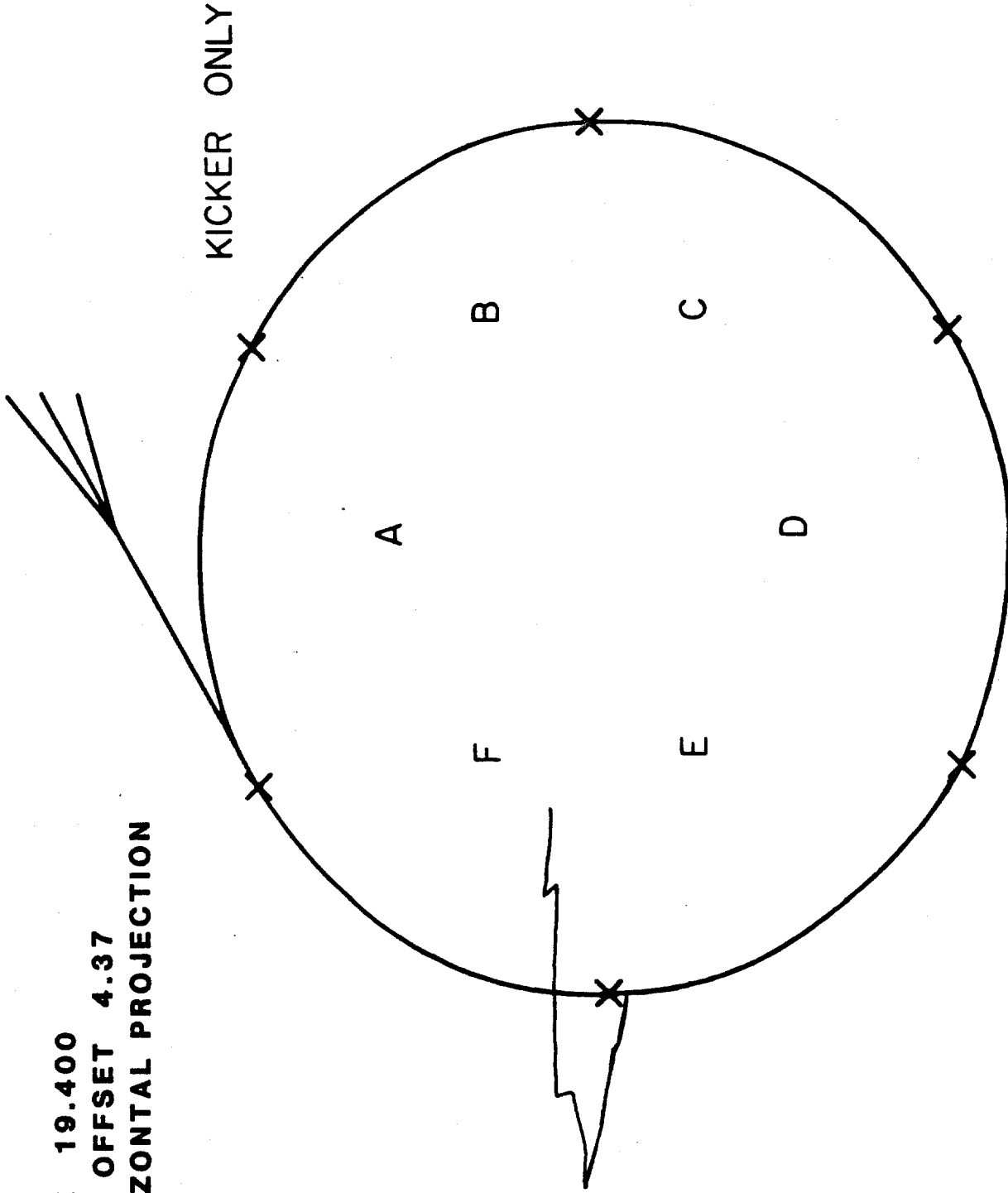


Figure 7-4

TUNE 19.400
MAX. OFFSET -4.19
HORIZONTAL PROJECTION

FØ 4 BUMP
+ KICKER

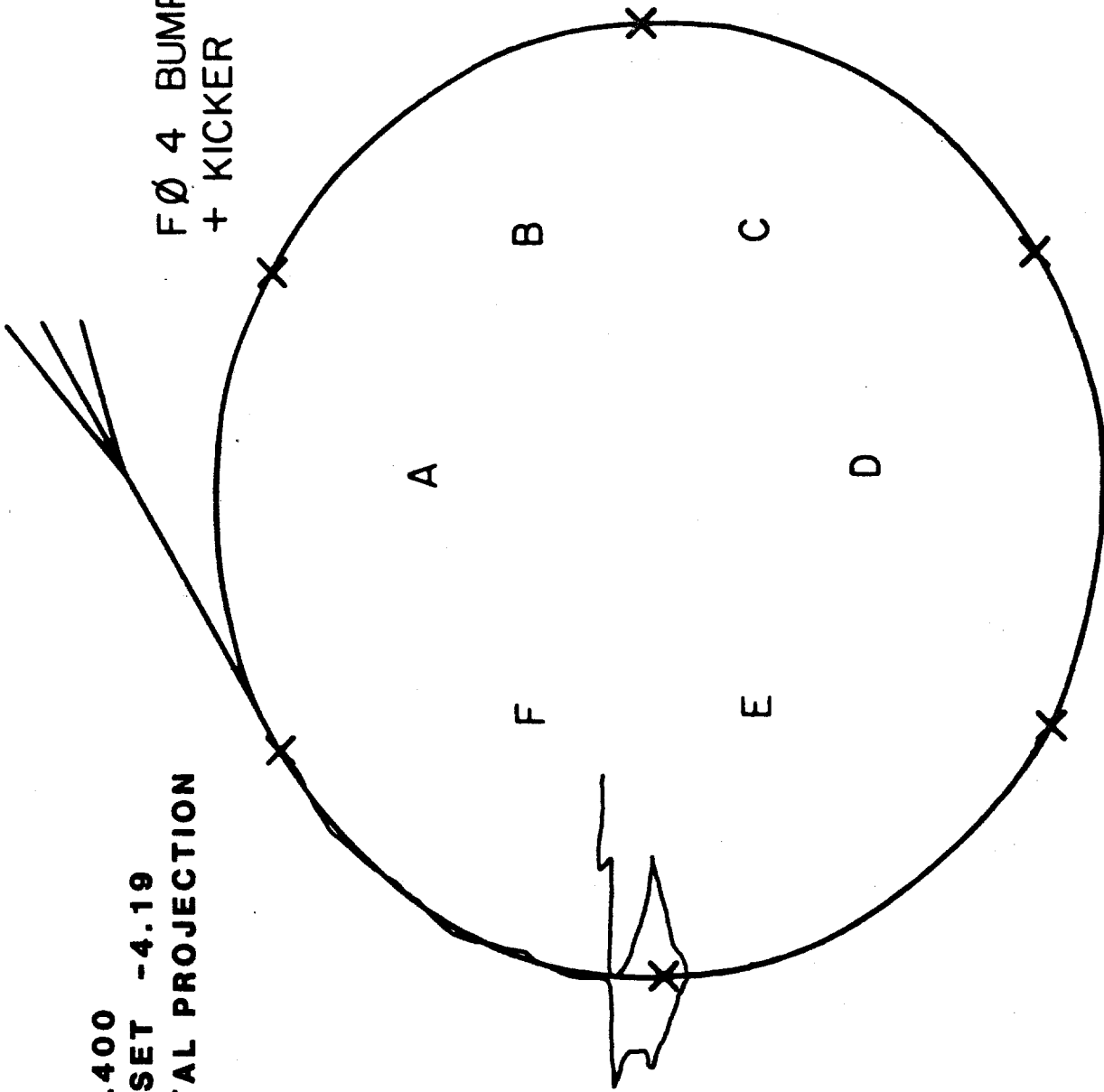


Figure 7-5

TUNE 19.400
MAX. OFFSET -4.33
HORIZONTAL PROJECTION

FØ 4-BUMP
F17 4-BUMP
KICKER

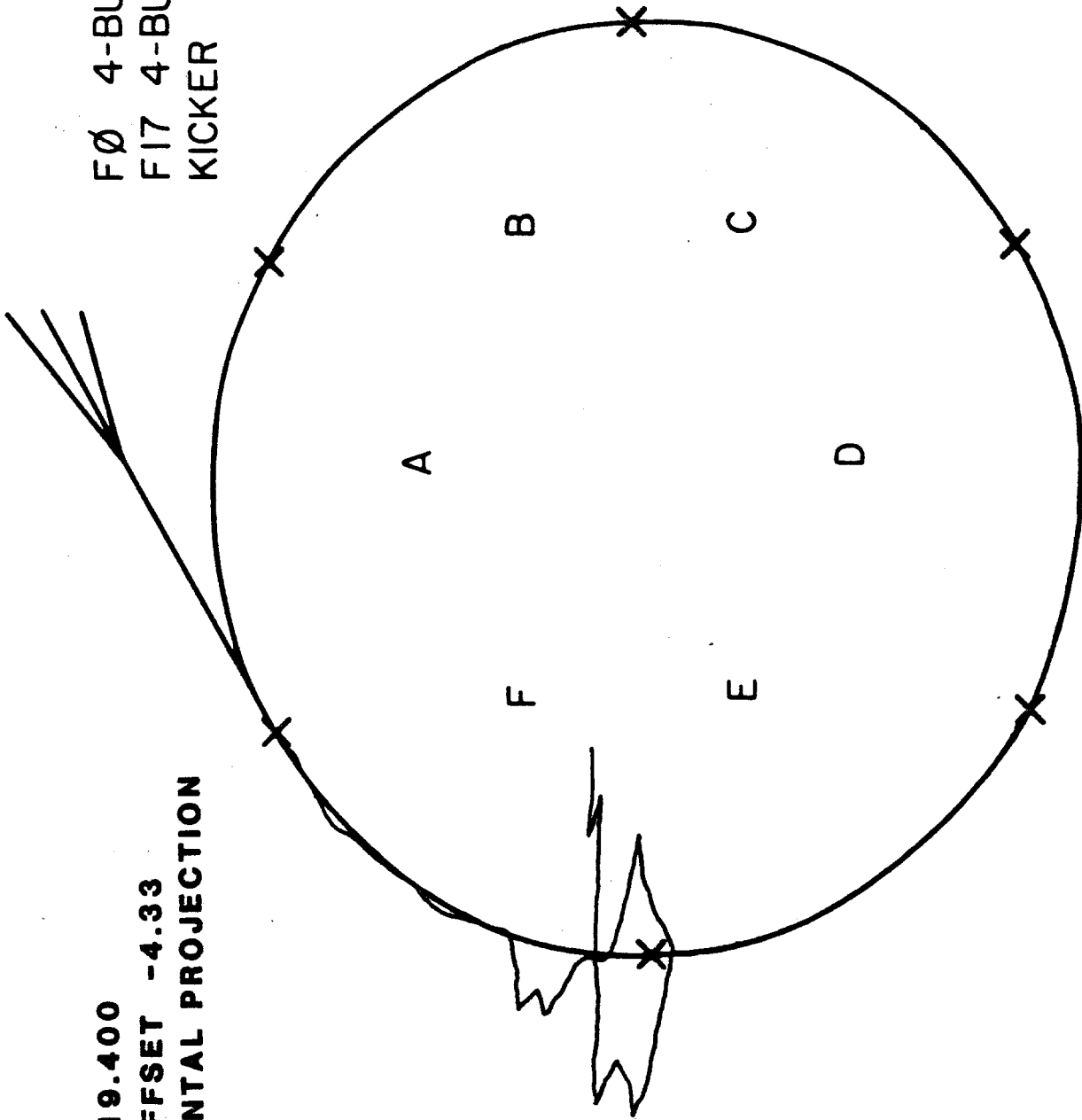
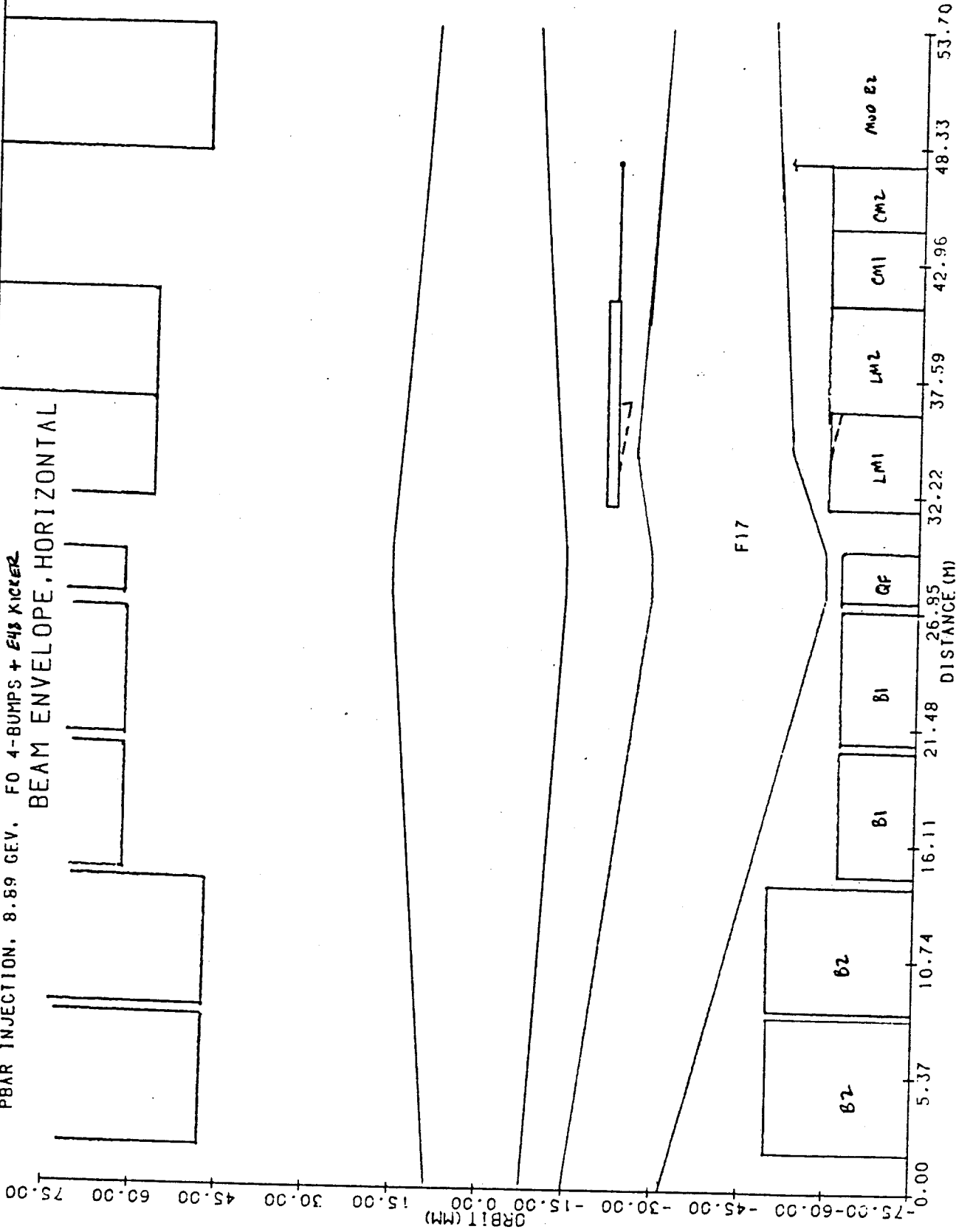


Figure 7-6

PBAR INJECTION, 8.89 GEV, FO 4-BUMPS + E48 KICKER
 BEAM ENVELOPE, HORIZONTAL



The injection angle required at F17 is 0.95 to 1.05 mrad (depending on the size of the F17 steering bump required.) The difference between this angle and the 0.8 mrad introduced by the rolled Lambertson can be achieved using the trim dipole in the AP1 line. In the worst case, this produces a 4 mm beam offset from the C-magnet center line, which is tolerable (see Fig. 7-1.)

7.3 Main Ring Acceleration and Rebunching Hardware

The processes of accelerating small groups of proton bunches and cooled antiprotons to 150 GeV has been described previously in Chapter 6. In those descriptions reference was made to an rf system in the Main Ring providing 22kV at $h = 53$ (2.529 MHz) and 3.7 kV at $h = 106$. This requirement will be met by installing two heavily ferrite-loaded rf cavities, each operating at the 20-kW level. These cavities will be refurbished and slightly modified cavities from the Princeton Pennsylvania Accelerator (PPA). Operation of these cavities in the Main Ring will require installation of an anode power supply of about 8 kV, 15 A (120 kW). Small additions to the low-level rf system will also be required to provide appropriate rf driving signals phase-locked to the integrally related $h=1113$ 53 MHz rf.

Small additions to the control system will also be required for remote operation of these systems.

7.4 Main Ring Overpass

The performance of both the Antiproton Source and the Collider Detector can be significantly improved by bypassing the Main Ring beam around the Collider Detector at B0. This bypassing - called here the "Overpass" - has at least two advantages:

- (i) It allows elimination of the asymmetric hole for the Main Ring through the Collider Detector;
- (ii) It allows accumulation of antiprotons to proceed simultaneously with colliding-beam operation. This will increase the average luminosity of the entire system by eliminating the pause of several hours while the antiproton beam is being refreshed.

The design of an overpass for the Main Ring, called TCB21, has been worked out in detail by T.L. Collins and is presented here. There are a number of constraints that such a design must satisfy:

- (a) Space must be generated for additional bending elements;

- (b) The new path must close smoothly on to the old path to high precision in both horizontal and vertical dimensions and at all energies with a minimum of programmed external control.
- (c) The path lengths must be the same in old and new paths, or differ by an integral number of rf wavelengths;
- (d) the betatron functions must match, as in any insertion; and
- (e) Any residual dispersion introduced outside the overpass must be small.

The overpass design limits Main Ring operation to 200 GeV or less. Some magnets are operated at twice the normal field. Consider a set of four bending magnets. The outer two magnets will be unchanged to provide the normal horizontal bend. The inner magnets will be rolled about the beam axis to produce a vertical bend of 32.3 mrad. Such four-magnet sets placed symmetrically around the long straight section (for example, at A41 and B12) will produce a 19 ft vertical separation, enough to miss the entire detector. The new orbit connects smoothly on both ends. A total of four sets (16 magnets) is in the additional circuit. The additional excitation of this circuit will be provided by a separate power supply.

Of sixteen special dipoles excited by a common power supply, eight for the vertical bending have (3"x3") aperture, while the remaining eight for the horizontal bending are essentially the same as the main ring B2 dipole with (2"x4") aperture but are modified to provide a field twice as large as the main bend field at the same excitation current.

The overpass has approximately 8 in. of extra orbit length. This undesired length is cancelled by combining the vertical bends with a slight inward bend to "cut across" the arc. The inward bend can be accomplished easily by rolling the vertical dipoles by 6.3°.

The betatron functions are easily matched across the insertion. The vertical dispersion introduced in the remainder of the ring must be balanced with some care. Its maximum value has been reduced by this balancing to approximately 0.5 m, which is noticeable, but tolerable. Coordinates of the overpass insertion magnets are given in Table 7-I and the maximum values of vertical dispersion around the ring are listed in Table 7-II. The locations of elements are shown in Fig. 7-8.

TABLE 7-I OVERPASS COORDINATES FOR TCB21

Numbers in parentheses are for the original Main Ring ($Z=\theta_v=0$).

Station	x(feet)	y(feet)	θ_h (rad)	Z(inches)	θ_v (rad)
A39	962.531 (962.531)	2,285.083 (2,285.083)	.8175454 (.8175454)	0.000	0.00000
A42	1,034.911 (1,034.808)	2,350.493 (2,350.639)	.8535781 (.850017)	19.286	.0322656
A43	1,109.464 (1,109.175)	2,413.368 (2,413.813)	.8860663 (.882488)	57.063	.0322656
A44	1,186.021 (1,185.554)	2,473.789 (2,474.539)	.9185544 (.914959)	94.840	.0322656
A45	1,264.500 (1,263.864)	2,531.691 (2,532.754)	.9510426 (.947430)	132.617	.0322656
A46	1,344.818 (1,344.023)	2,587.013 (2,588.396)	.9835307 (.979902)	170.393	.0322656
A47	1,426.890 (1,425.946)	2,639.697 (2,641.406)	1.0160189 (1.012373)	208.180	.0322656
A48	1,510.566 (1,509.547)	2,689.860 (2,691.728)	1.00448499 (1.044844)	226.656	.0000000
B0	1,686.376 (1,685.357)	2,787.887 (2,789.756)	1.0692033 (1.069198)	226.656	.0000000
B11	1,772.743 (1,771.723)	2,835.248 (2,837.117)	1.0692033 (1.069198)	226.656	.0000000
B12	1,870.616 (1,869.596)	2,887.172 (2,889.042)	1.1016746 (1.101669)	226.656	.0000000
B13	1,958.274 (1,957.352)	2,929.994 (2,931.709)	1.1304914 (1.134140)	207.364	-.0322641
B14	2,047.177 (2,046.446)	2,970.092 (2,971.504)	1.1629795 (1.166611)	169.589	-.0322641
B15	2,137.335 (2,136.786)	3,007.281 (3,008.386)	1.1954677 (1.199083)	131.815	-.0322641
B16	2,228.654 (2,228.275)	3,041.523 (3,042.315)	1.2279558 (1.231554)	94.040	-.0322641

B17	2,321.037 (2,320.818)	3,072.779 (3,073.256)	1.2604440 (1.264025)	56.625	-.0322641
B18	2,414.047 (2,413.981)	3,102.116 (3,102.275)	1.2766880 (1.280261)	18.491	-.0322641
B19	2,507.920 (2,507.920)	3,128.673 (3,128.673)	1.3127319 (1.312732)	.000	.0000000

TABLE 7-II. VERTICAL DISPERSION AT $\beta_v = 100\text{m}$ WITH THE B0 OVERPASS TCB21

	$v = 19.40$	$v = 19.60^*$
outside	0.51m	0.34m
A39 - A47	2.58	2.30
A47 - B12	4.68	4.39
B12 - B19	2.55	2.25

*The tune of 19.40 is the standard value for the fixed-target run while 19.60 might be preferable for the storage mode of operation.

7.5 Main Ring Diagnostics

7.5.1 Main Ring Position Detectors. The electronics used to read out the position of the Main Ring beam will be improved to have capabilities similar to the Energy Saver position detectors described in Sec. 8.6.1. This improvement is needed for commissioning the p system. Orbit information is necessary at both $h=53$ and $h=1113$ for both protons and antiprotons in the Main Ring.

7.6 D0 Overpass

A second Main Ring overpass will be built at D0 for the same purpose as the B0 overpass: to bypass the Main Ring beam around the detector or detectors. The D0 overpass is planned to minimize tunnel modifications. The maximum possible height under this restriction is 63.7 in. from the present Main Ring beamline or a clearance of 63.7 in. + 25.5 in. = 89.2 in. over the Tevatron center line.

One vertical dipole (instead of two for the B0 overpass) and two special horizontal dipoles are needed at each of two outer bend locations. At two inner bend locations, we need only vertical dipoles, one at each location. In order to achieve the maximum possible separation of 89.2 in., two outer bends should be at C46-2 and D13-5. Two inner bends are within the D0 longstraight and the clear space at D0 along the beamline for the detector is 32 ft upstream and 37.8 ft downstream from D0. This design is called WD89. Unlike TCB21 at B0, the D0 overpass has been designed without any attempt to localize the vertical dispersion within the overpass. As a

consequence, the maximum vertical dispersion outside the overpass can be as large as 2m at $\beta_v = 100\text{m}$ when the B0 overpass is also installed. In order to find out how much the momentum and transverse acceptances are affected with such a large vertical dispersion around the ring, we will install a test overpass, called WD51, during the shutdown in July, 1984. The beam height of this overpass is 51.15 in. from the present Main Ring beamline and the outer bends are at C46-4 and D13-3, while the inner vertical bends are in the D0 long straight section. They are as far apart as possible in order to prevent the overpass line from penetrating the tunnel ceiling. Although the height is not as much as in WD89, the maximum vertical dispersion is approximately 1.7m around the ring. Later, by simply moving two inner vertical dipoles to the location specified in WD89, we can increase the beam height to 81.3 in. from the Tevatron beamline. This version, called WD81, keeps all other magnets in the same positions as in WD51. At present, the design of detectors at D0 is still in progress and the final choice between WD81 and WD89 cannot be made. For WD89, most magnets inside the overpass must be moved from the position specified for the test overpass WD51. The maximum vertical dispersions at $\beta_v = 100\text{m}$ for various cases are listed in Table 7-III. The locations of all the elements of the two bypasses are shown in Fig. 7-8.

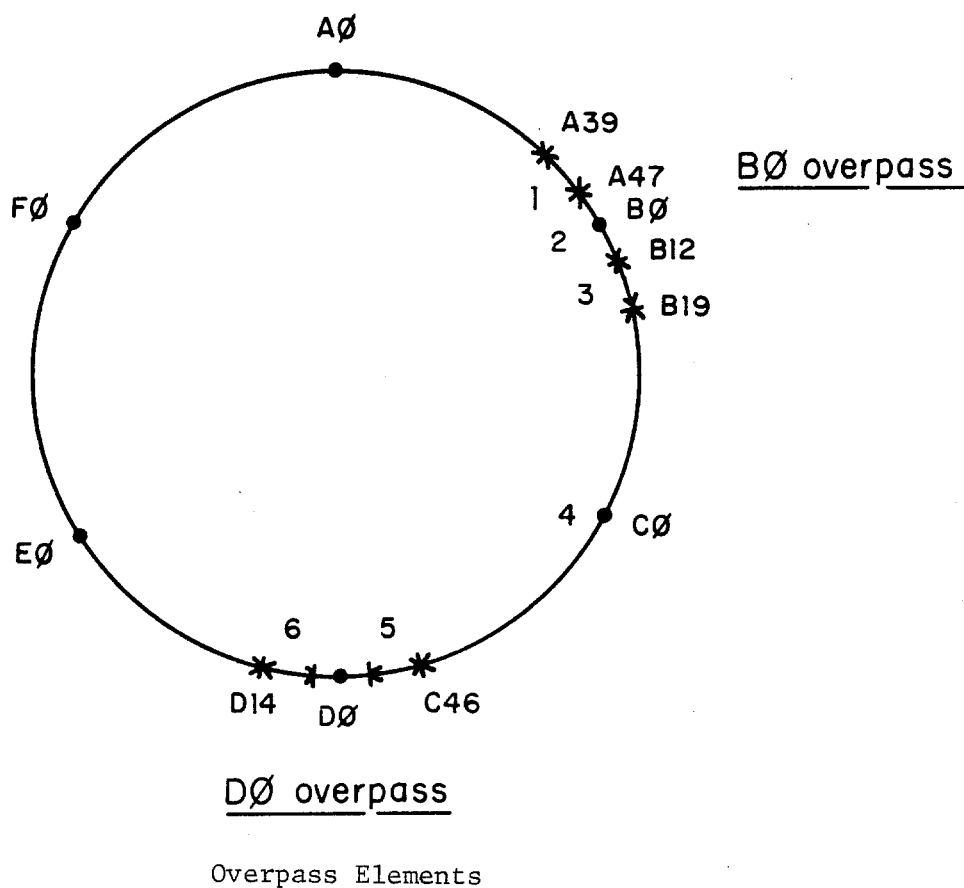


Figure 7-8

TABLE 7-III VERTICAL DISPERSIONS IN EACH REGION (normalized at $\beta_v = 100m$)

		outside	"1"	"2"	"3"	"4"	"5"	"6"
fract. =		60.4%	2.8%	2.5%	3.3%	27.1%	1.9%	1.9%
length								
	tune							
(A)	19.40	<-----	-----	1.67m	-----	---->	1.42m	1.52m
(B)	19.40	1.16	2.12	4.43	2.97	2.12	1.91	1.15
	19.60	1.38	2.20	4.48	3.02	2.03	2.34	1.91
(C)	19.40	1.46	2.50	4.79	3.38	2.43	2.04	0.90
	19.60	1.65	2.61	4.88	3.45	2.29	2.34	1.92
(D)	19.40	0.51	2.58	4.68	2.55	<-----	0.51 -	---->
	19.60	0.34	2.30	4.39	2.25	<-----	0.34 -	---->

(A) WD51 alone (B) TCB21 and WD81 (C) TCB21 and WD89 (D) alone.